Climate Dynamics (2023) 61:399–412
https://doi.org/10.1007/s00382-022-06592-8

Combined impact of ENSO and Antarctic Oscillation on austral spring precipitation in Southeastern South America (SESA)

Xinjia Hu[1] · Jan Eichner[2] · Daoyi Gong[4,5,6] · Marcelo Barreiro[3] · Holger Kantz[1]

Received: 16 July 2022 / Accepted: 10 November 2022 / Published online: 19 November 2022
© The Author(s) 2022

Abstract
Southeastern South America (SESA)'s precipitation is thought to be influenced by both El Niño Southern Oscillation (ENSO) and Antarctic Oscillation (AAO), especially in austral spring. Previous studies conclude AAO can modulate ENSO's impact on precipitation over the SESA region without differentiating between El Niño and La Niña events. In the present study, we use composite analysis to further explore the combined impact of AAO and ENSO on austral spring precipitation over Southeastern South America (SESA) to answer this question and explain the dynamic mechanisms. We found that different AAO phases can influence La Niña's impact on SESA austral spring precipitation considerably, while this does not apply for El Niño events. From our analysis, we found that AAO exerts more impact on austral spring precipitation over SESA compared to ENSO during La Niña years by influencing northerly wind and southward water vapor flux, which contributes most of the moisture into the SESA region, due to the strengthening of South Atlantic subtropical anticyclone and stronger meridional gradient in low-level pressure. Besides, there is an upper-level trough (ridge) over subtropical South America indicating advection of cyclonic (anticyclonic) vorticity inducing anomalous increase (decrease) of precipitation over that region during La Niña/AAO− (La Niña/AAO+). We do not see this opposite difference within El Niño groups combined with different phases of AAO.

Keywords ENSO · AAO · Southeastern South America · Precipitation · Teleconnection

1 Introduction

The southeastern South American region (SESA, the subtropical region east of the Andes, roughly between 45° –65° W, 20°–40° S) is one of the AR6 WGI reference regions, which is used as an illustration of the interplay between climate variability drivers and regional change. This area covers the most active agricultural region and is one of the most populated parts in South America (Olmo and Bettolli 2022), extending over Uruguay, Paraguay, southern Brazil and eastern Argentina. This region is especially susceptible to extreme precipitation as part of the La Plata River Basin, which strongly depends on agriculture and hydroelectricity production (Zamboni et al. 2010; Nuñez and Blázquez 2014).

SESA is one of the rainiest portions of the continent and one of the few areas in the world where an obvious increasing trend of precipitation has been detected since the 20th century (Olmo et al. 2020; Díaz et al. 2021), mainly in the austral late spring and summer (Gonzalez et al. 2014). Precipitation in SESA has large variability from interannual

✉ Xinjia Hu
xinjia@pks.mpg.de

1 Max Planck Institute for the Physics of Complex Systems, Nöthnitzer Str. 38, 01187 Dresden, Germany

2 Munich Reinsurance company, Königinstr. 107, 80802 Munich, Germany

3 Departamento de Ciencias de la Atmosfera, Facultad de Ciencias, Universidad de la Republica, Igua 4225, 11400 Montevideo, Uruguay

4 State Key Laboratory of Earth Surface Processes and Resource Ecology (ESPRE), Beijing Normal University, Beijing, China

5 Key Laboratory of Environmental Change and Natural Disasters, Ministry of Education, Beijing Normal University, Beijing, China

6 Faculty of Geographical Science, Beijing Normal University, Beijing, China

to multidecadal time scales, which has significant impacts on agricultural and socio-economic aspects (Martín-Gómez and Barreiro 2016). There are significant signals of El Niño Southern Oscillation (ENSO) on the annual variation of precipitation in SESA (Grimm et al. 2000; Barros and Silvestri 2002; Silvestri 2005; de Souza et al. 2021). Previous research shows that ENSO is significantly positively correlated with the precipitation variation in SESA, and this correlation is most robust and strongest in austral spring while weaker in austral summer (Montecinos et al. 2000; Barreiro 2010). Grimm et al. (1998) found that in November(0) of El Niño (EN) years, there occur the highest precipitation anomalies due to the intensification of the mesoscale convection, and vice versa during La Niña (LN) years. This relationship serves as the foundation of using ENSO as an interannual predictor of precipitation in that region (Zamboni et al. 2010).

Other factors can modulate ENSO's impact on precipitation in the SESA region. It is found that the precipitation variability during OND among El Niño events is modulated by SST in the subtropical south-central Pacific (SSCP) (Barros and Silvestri 2002). This means that the response of precipitation to EN events or LN events might be different, which may be caused by the difference in intensity or evolution of different EN/LN events, while it can also be associated with other regional or remote forcings. Silvestri and Vera (2003) detected that the Antarctic Oscillation (AAO) has a strong modulation of ENSO's impact on SESA precipitation during austral spring based on correlation analysis (Silvestri and Vera 2003). In the Southern Hemisphere, AAO is the dominant pattern of circulation anomaly variability (Thompson and Wallace 2000) and is characterized by a large-scale seesaw oscillation of atmospheric masses between mid-latitudes and the Antarctic (Gong and Wang 1999). It is the basic structure of atmospheric circulation in the Southern Hemisphere and shows the variation of the intensity of the mid-latitude westerlies in the Southern Hemisphere (Qin et al. 2005). There is anomalously low pressure over Antarctica and high pressure over the mid-latitudes of the Southern Hemisphere during the positive phase of the AAO and vice versa. These patterns can be found throughout the year; however, AAO is more active during austral spring (Gong and Wang 1999; Thompson and Wallace 2000). Silvestri and Vera (2003) explored the combined effect of ENSO and AAO on precipitation over SESA by correlation analysis. They concluded that variation of AAO strongly modulates precipitation in the SESA region because it explains the variance fraction of precipitation not related to ENSO. However, correlation analysis may not be sufficient to figure out the combined impact considering the decadal variation of AAO–ENSO relationship (Fogt and Bromwich 2006; L'Heureux and Thompson 2006; Stammerjohn et al. 2008). Additionally, whether the impacts of AAO are the same among EN events or LN events is unknown.

Considering that precipitation anomalies can cause severe impacts on human society and economics, especially over the regions strongly dependent upon agriculture and hydroelectricity production, such as SESA (Zamboni et al. 2010), it is meaningful to explore the combined impact of ENSO and AAO on precipitation anomalies over the SESA region and provide suggestions for decision-makers to make effective response. In this study, we use composite analysis to explore the teleconnection of both climate variabilities and analyze whether the modulation of AAO on ENSO's impact is linear or nonlinear. Because the connection between ENSO and AAO is obvious in the seasons when the ENSO phases reach their mature stage, namely austral spring and summer (Fogt and Bromwich 2006), and AAO is most active in austral spring (Han et al. 2017), in this study, we explore the role of the combined impact of AAO and ENSO on SESA precipitation in austral spring and the physical processes behind it.

2 Data and methodology

In this study, we focus on the period between 1979–2019 (all datasets we used cover this period), considering the quality of reanalysis data in the Southern hemisphere is improved substantially since 1979 with coverage by satellites. We use four monthly observational precipitation datasets and one reanalysis precipitation dataset to check the robustness of our results. The Global Precipitation Climatology Project's (GPCP v2.3) precipitation dataset is the combination of satellite data and observations with a resolution of 2.5° (Adler et al. 2018). The second dataset is the CPC Merged Analysis of Precipitation (CMAP), with the same spatial resolution as GPCP (Xie and Arkin 1997). NOAA/OAR/ESRL PSL provides GPCP and CMAP from their website. The third dataset is the Global Precipitation Climatology Center (GPCC) full data monthly product (version 2020), which is the land precipitation estimate only based on station data, and this dataset is available in the 0.5° resolution (Schneider et al. 2008, 2017, 2020). The fourth observational dataset is from the Climate Research Unit (CRU TS v.4.06) with a spatial resolution of 0.5° (Harris et al. 2020). We also use the reanalysis of monthly precipitation from the fifth-generation European Center for Medium Range Forecasts (ECMWF) reanalysis (ERA5) (Hersbach et al. 2020). Great caution needs to be approached when using reanalysis precipitation data because reanalysis products usually have large variations. However, compared to satellite datasets, reanalyses agree better with in situ observations over extra-tropical land areas, although tending to fall into 'wet' and 'dry' sets generally (Alexander et al. 2020). Outgoing Longwave Radiation (OLR) measures the amount of terrestrial longwave radiation released into

space. By extension, it can be intercepted by water vapor and cloud in the atmosphere. Negative (positive) OLR anomaly indicates enhanced (suppressed) convection. Therefore OLR can be used as a proxy for precipitation. We use monthly interpolated Outgoing Longwave Radiation (OLR) data from NOAA (Liebmann and Smith 1996).

We use the vertical integral of northward water vapor flux (IVT, positive values indicate a flux from the south direction to the north, negative represents the water vapor flux transported from the north) and the vertical integral of eastward water vapor flux (IVT, positive values indicate a flux from west to east and vice versa) from ERA5 monthly averaged data on the single level dataset, which is vertically integrated from the surface of the Earth to the top of the atmosphere (Hersbach et al. 2019). Monthly mean atmospheric datasets including geopotential horizontal wind, geopotential height in this paper come from the ERA5 monthly averaged data on pressure levels dataset. The monthly intrinsic pressure level stream function is from NOAA NCEP/NCAR Climate Data Assimilation System I (CDAS-1) dataset (Kalnay et al. 1996). All anomalies in this study are calculated with regard to the climatological bimonthly mean based on the period 1979–2019.

We use the monthly Southern Annular Mode (SAM) index defined by Marshall to represent AAO (available from http://www.nerc-bas.ac.uk/icd/gjma/sam.html) (Marshall 2003). It is based on the differences between normalized monthly zonal mean sea level pressure (MSLP) at 40 °S and 65° S following the definition of Gong and Wang (Gong and Wang 1999). SAM is slightly altered because it uses the mean MSLP observations from six stations located approximately at each of the latitudes to calculate a proxy zonal mean (Marshall 2003). ENSO events are represented by the Niño 3.4 index, which is defined as the SST anomalies in the Niño 3.4 region (170° W–120° W, 5° S–5° N) and is available from the Climate Prediction Center (CPC, https://psl.noaa.gov/data/climateindices/list/). Both indices are linearly detrended and standardized prior to analysis. A composite analysis is applied in this study to explore the combined influence of ENSO and AAO on precipitation anomalies over SESA. We assess the statistical significance of the composite anomalies by a Student's *t* test.

3 Results

3.1 Climatological features of SESA

Prior to analyzing the combined impact of ENSO and AAO on precipitation over SESA, we first describe the climatological precipitation and atmospheric circulations in SESA. In southeastern South America, precipitation presents large variability from interannual to multidecadal time scales and is influenced by tropical oceans (Martín-Gómez and Barreiro 2016). We calculate the mean bimonthly precipitation over the SESA region for each of our five datasets. Figure 1a shows that precipitation in SESA is the strongest in austral spring (ND) and summer (JF). In this study, we focus on the austral spring (ND) precipitation because previous research indicated that the link between precipitation over SESA and ENSO is the strongest in austral spring as well as AAO is most active in this season (Grimm et al. 2000; Barreiro 2010; Martín-Gómez and Barreiro 2016).

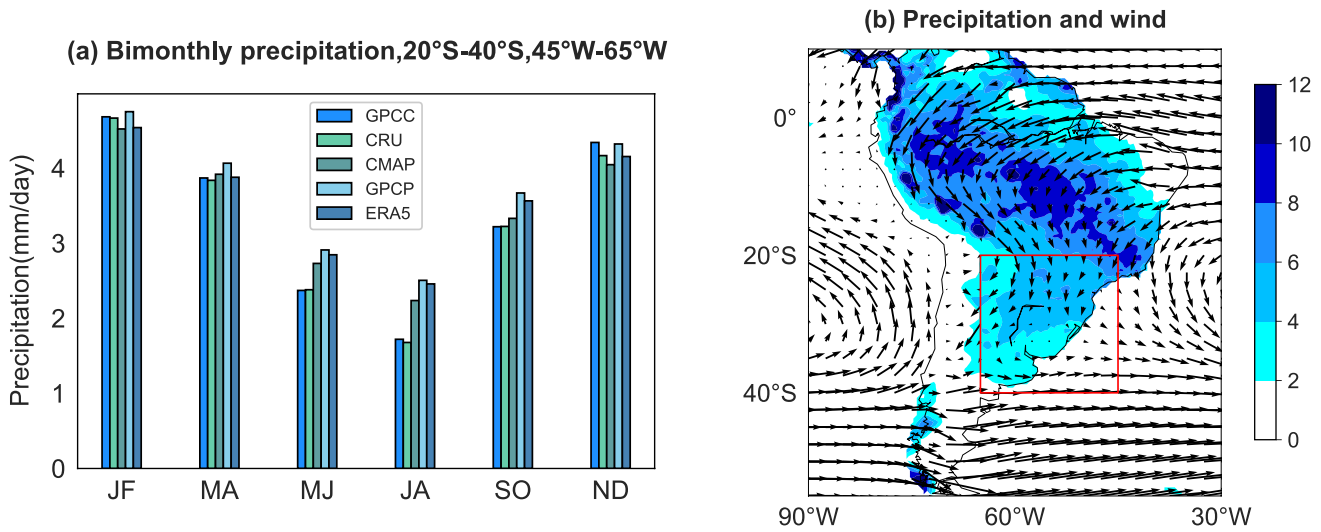

Fig. 1 **a** Climatological mean of bimonthly precipitation over the SESA region during 1979–2019 (unit: mm/day). **b** Climatological mean of precipitation (shading, unit: mm/day, using GPCC precipitation dataset) and 850 hPa horizontal wind of ND season during 1979–2019 (vectors, unit: m/s)

We use all the precipitation datasets mentioned above to plot the climatological mean of precipitation in the ND season during 1979–2019 over the SESA region and find no noticeable difference among all the datasets. Therefore we use the result from the GPCC dataset as an example in Fig. 1b, as the GPCC dataset is the precipitation estimate only based on station data and has higher spatial resolution among all the datasets we used. Figure 1b describes climate means of precipitation and 850 hPa horizontal wind in the months ND. An easterly flow at low latitude from the tropical ocean turns south after getting close to the Andes, transporting heat and moisture to subtropics. Generally, the strengthening of the low-level northerly flow along the eastern side of the Andes indicates the South America low-level jet (SALLJ) events. The SALLJ determines the spatio-temporal variability of precipitation in SESA because it transports a large amount of moisture from the Amazon basin to this region. Previous research concludes that the frequency of SALLJ is significantly modulated by ENSO, especially during austral spring (Montini et al. 2019). To the south of 40° S, mean conditions are dominated by a westerly low-level flow, which persists throughout the year and is accompanied by typical mid-latitude perturbations. In summary, low-level northerly and moisture from the north of South America and the Amazon are crucial for precipitation in SESA. In this study, we explore the impact of AAO and ENSO on austral spring precipitation over SESA and analyze the circulation anomalies (low-level horizontal wind, geopotential height, and 200 hPa streamfunction) and water vapor transport related to AAO and ENSO. Additionally, we discuss the frequency variation of SALLJ events among different groups in the discussion section.

3.2 Extreme ENSO and AAO cases

Previous research indicates that AAO is on average anti-correlated with ENSO, especially at interannual time scale during late austral spring and austral summer (L'Heureux and Thompson 2006; Clem and Fogt 2013; Vera and Osman 2018) and more significantly in recent decades (Vera and Osman 2018). There is a preference for the occurrence of AAO negative phase during El Niño events and AAO positive phase during La Niña events (Clem and Fogt 2013), in which cases ENSO teleconnection reinforces due to the increase of transient momentum flux in the South Pacific (Fogt et al. 2011). However, there also exist outliers, when El Niño is associated with unusual AAO positive phase, for example, the El Niño year 2015/16 (Fogt and Bromwich 2006; Vera et al. 2018) when AAO and ENSO are out-of-phase.

The scatter diagram of the ENSO-AAO-index distribution is presented in Fig. 2 based on the detrended and standardized indices of the ND seasonal mean of both indices.

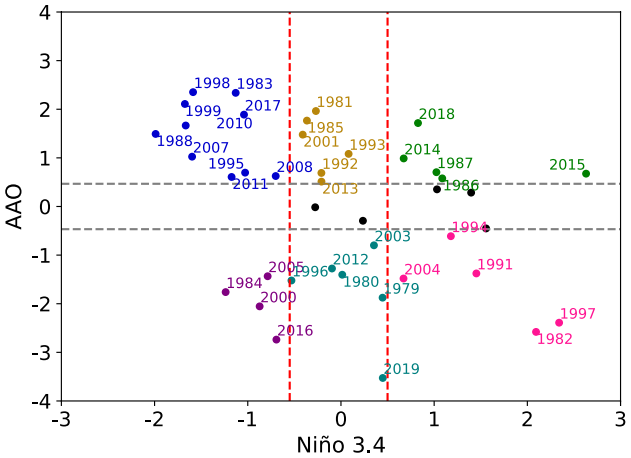

Fig. 2 Scatter diagram between SAM index and Niño 3.4 index for ND (red dashed lines indicate thresholds for separating La Niña, ENSO neutral and El Niño events; Grey dashed lines are the thresholds for defining positive and negative AAO phases; Different colors of the dots represent differing classifications consistent with Table 1; Black dots represent years in AAO neutral phase, which are out of our interest)

To ensure the sample size for composite analysis, we select ± 0.3 standard deviations as the threshold to define positive/negative phases of AAO. For ENSO events, we use the value ± 0.5 to separate El Niño and La Niña events. The events which are outside of the thresholds can be divided into two groups, namely "in-phase" events (both indices are beyond the threshold and of opposite sign, including El Niño/AAO− and La Nina/AAO+) and "out-of-phase events" (both indices are over threshold and of the same sign, including El Niño/AAO+ and La Niña/AAO−). Although in each of the four sub-groups, there exist several events, we could see clearly that the in-phase events occur more often than out-of-phase events, indicating the fact that El Niño events preferentially come with AAO− and La Niña events occur preferentially with AAO+, which are mentioned by previous studies (Fogt and Bromwich 2006; L'Heureux and Thompson 2006; Gong et al. 2010; Clem and Fogt 2013). In this study, we define ENSO neutral phases combined with positive/negative AAO phase as well, i.e., ENSO neutral/AAO+ and ENSO neutral/AAO−, which will be used to study AAO's impact without ENSO's influence.

Based on the above classification, we obtained six groups in total, which are from the ENSO phases in 1979–2019, combined with different AAO phases shown in Table 1.

3.3 Austral spring precipitation anomalies in SESA

Precipitation over SESA is significantly positively correlated with ENSO during austral spring (Montecinos et al. 2000), the season during which the most robust relationship between ENSO and SESA precipitation is found (Barreiro

Table 1 Classification of springs based on the phases of ENSO and AAO during 1979–2019

Case	AAO+	AAO−
El Niño	1986, 1987, 2014, 2015, 2018	1982, 1991, 1994, 1997, 2004
La Niña	1983, 1988, 1995, 1998, 1999, 2007,2008, 2010, 2011, 2017	1984, 2000, 2005, 2016
ENSO neutral	1981, 1985, 1992, 1993, 2001, 2013	1979, 1980, 1996, 2003, 2012, 2019

2010). It is thought that the teleconnection of ENSO is essentially linear, indicating that El Niño and La Niña tend to generate opposite precipitation anomalies, where precipitation tends to be higher during El Niño events while having the opposite effect during La Niña years (Ropelewski and Halpert 1987; Rao and Hada 1990). This is supposed to be the basis for the predictability of precipitation in this region (Grimm et al. 2000; Zamboni et al. 2010). Additionally, it is noticed that precipitation anomalies among different EN (LN) events are sometimes greater than the mean difference

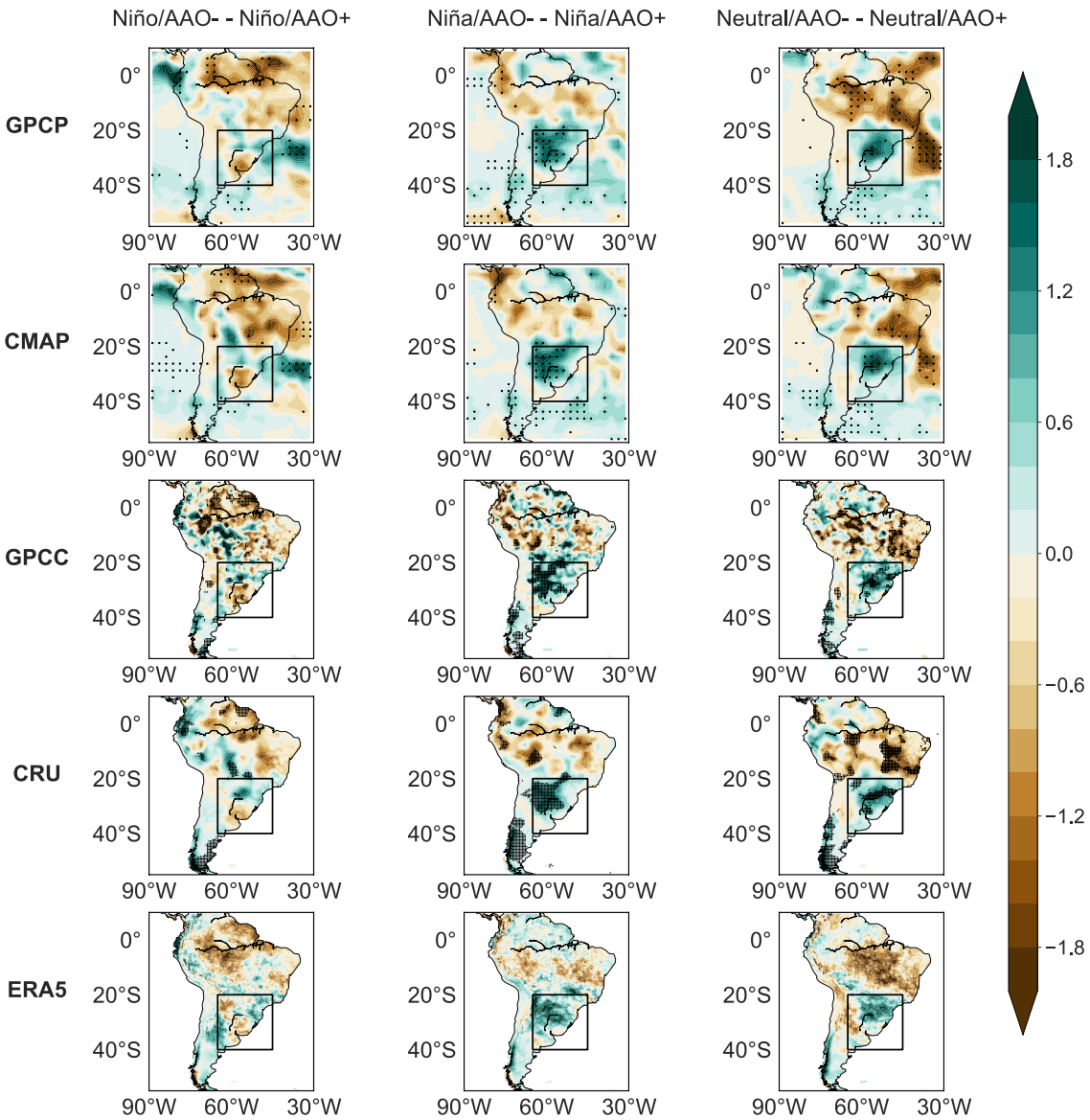

Fig. 3 Differences of precipitation composites (unit: mm/day) in ND based on different groups in Fig. 2; The dotted regions indicate statistical significance at the 95% confidence level estimated by two-tailed Student's *t* test (from top to bottom: using monthly precipitation dataset GPCP, CMAP, GPCC, CRU, ERA5)

between different phases of ENSO (Barros and Silvestri 2002).

In order to explore whether AAO has similar impacts on EN and LN events on austral spring precipitation anomalies over SESA, we apply a composite analysis with a significance test at 95% level, based on different groups identified in Fig. 2. We use and compare all five precipitation datasets for the analysis of the ND-precipitation composite anomalies and obtain the Fig. 3. It illustrates the following results, which are confirmed by each of the datasets: (1) AAO has an impact on austral spring precipitation over this region, with more precipitation during AAO negative phases and vice versa, indicated by the difference in precipitation composites between ENSO neutral years combined with AAO negative and positive phases. This confirms the conclusion obtained by Silvestri and Vera that there exists a negative correlation between AAO and precipitation over Paraguay and adjacent regions in ND season (less precipitation during AAO positive phase) (Silvestri and Vera 2003). There is a dipole pattern of precipitation between the SESA area and the SACZ region due to the influence of the Pacific-South America (PSA) patterns and AAO, which is also found in previous research (Mo and Paegle 2001; Vasconcellos and Cavalcanti 2010). (2) AAO shows its apparent modulation on La Niña's impact on precipitation over SESA, especially in Paraguay, southeastern Brazil, northwestern Uruguay, and northeastern Argentina, indicating that when La Niña events occur combined with AAO negative phase, it causes less dry conditions compared with La Niña events during AAO positive phases (illustrated by the difference between two groups Niña/AAO− and Niña/AAO+, the middle column in Fig. 3). It means that not all La Niña events cause very dry conditions in the SESA region, while there exists a significant difference between La Niña events combined with different phases of AAO. (3) AAO does not show very significant modulation on El Niño's impact on austral spring precipitation over this region (represented in the precipitation difference between Niño/AAO− and Niño/AAO+, the left column in Fig. 3). Previous research from Silvestri and Vera explores the effect of ENSO and AAO on austral spring precipitation over SESA, using correlation analysis, with the conclusion that regions including northeastern Argentina, eastern Paraguay, and southern Brazil are influenced by the combined impact, while other parts of Argentina and Uruguay are influenced by ENSO with more independence of AAO variations (Silvestri and Vera 2003). However, their research does not distinguish the difference between AAO phases combined with El Niño and La Niña events. Our more detailed analysis shows that there exists this nonlinear response of ENSO events to AAO events, with different impacts of AAO on El Niño and La Niña events.

3.4 Water vapor transport

Identifying moisture variation is crucial to understand the variability of precipitation. Section 3.3 shows that austral spring precipitation in the SESA region is related to the combined effect of ENSO and AAO. These large-scale phenomena are responsible for atmospheric circulation system anomalies, which in turn influence the convective activity and moisture supply (Satyamurty et al. 2013). To explore moisture variation, we first calculate the moisture flux into the SESA region and the convergence of moisture over this area. The vertically integrated flux of water vapor is defined as follows:

$$\overrightarrow{Q} = g^{-1} \int_{P_t}^{P_s} (q\overrightarrow{V}) \mathrm{d}p \tag{1}$$

where q indicates specific humidity, $\overrightarrow{V}$ is the wind vector, p is pressure (P_s and P_t are the atmospheric pressures at the ground surface and top of the troposphere, respectively), and g is the acceleration caused by gravity. We use the monthly vertically integrated northward (meridional) water vapor flux (IVT) and vertically integrated eastward (zonal) water vapor flux (IVT) from the ERA5 dataset to calculate the amount of water vapor transported into the SESA region at the meridional and zonal direction. ERA5 defines these two parameters the horizontal rate of flux of water vapour, in the meridional and zonal direction, for a column of air extending from the surface of the Earth to the top of the atmosphere per meter across the flow. The mean convergence of the water vapor flux over the SESA region can be calculated by box model calculation (Satyamurty et al. 2013). We define the SESA region as a rectangle area (45°–65° W, 20°–40° S, in Fig. 1b). We calculate the convergence in meridional direction and zonal direction separately following:

$$Tr_{zonal} = \int_0^x \overrightarrow{Q} \mathrm{d}x \tag{2}$$

$$Tr_{meridional} = \int_0^y \overrightarrow{Q} \mathrm{d}y \tag{3}$$

where Tr_{zonal} and $Tr_{meridional}$ are the moisture transported across the boundaries into the SESA rectangular region. We take four boundaries of the SESA area, i.e., the western boundary (20°–40° S, 65° W) and eastern boundary (20° –40° S ,45° W) to calculate zonal transport of moisture into the SESA region; we take the northern boundary (45° –65° W, 20° S) and southern boundary (45°–65° W, 40° S) to calculate meridional moisture transport. The sum of transport in both directions is this region's total (net) vertically integrated water vapor flux convergence. We calculate these parameters in each group divided in Fig. 2. Figure 4

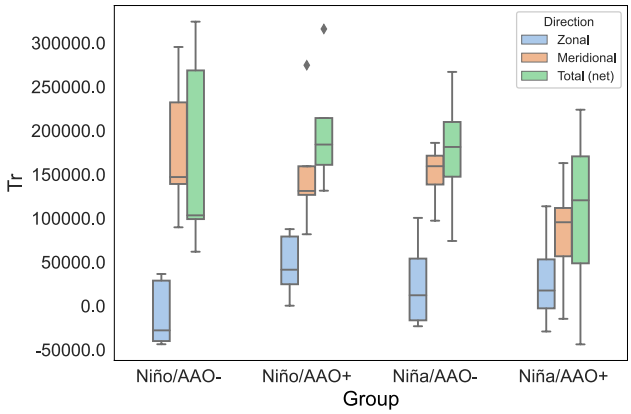

Fig. 4 Moisture transport across the zonal boundary and meridional boundary of the SESA rectangular area (unit: kg s^{-1}, calculated by the box model; positive numbers are moisture transported into the region and negative values are moisture transported out of the region)

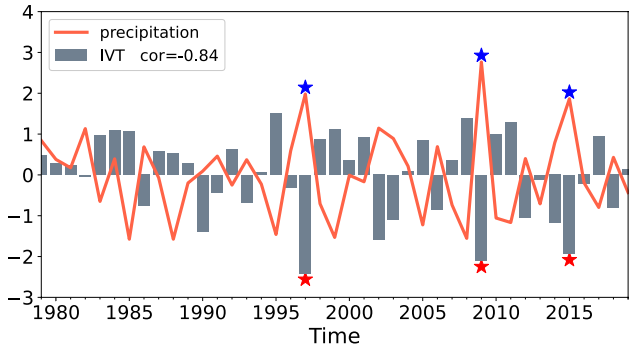

Fig. 5 Normalized time series of precipitation and vertical integral of northward water vapor flux (IVT) in the SESA region during ND from 1979–2019 (Extreme high precipitation and IVT in the same year are marked by stars)

illustrates that water vapor transport in the meridional direction contributes the largest amount of moisture convergence in the SESA area in all groups. The average of meridional moisture transport in the La Niña/AAO− group is more extensive than La Niña/AAO+ group (see in Fig. 4). We calculate the cross-correlation coefficient between moisture transport in both directions and precipitation in the SESA area during austral spring. The cross-correlation coefficient between moisture zonal transport and precipitation is 0.14, while the correlation coefficient between moisture meridional transport and precipitation is 0.79. Virji found that a northerly/northwesterly low-level jet (LLJ) east of the Andes is an important mechanism providing moisture to higher latitudes by using satellite data (Virji 1981). Salio et al. (2002) concluded that the moisture transported by the LLJ east of the Andes can influence the convective activity over northern Argentina and southern Brazil. From our analysis, we also confirm that water vapor transport in the meridional direction contributes most of the moisture transport in this region.

We use the monthly vertical integrated northward water vapor flux (IVT) from the ERA5 dataset to calculate the climatology (in supplementary material, Fig. S1) and anomalies of regional mean IVT in the meridional direction in austral spring. The climatology is negative, illustrating that the moisture is transported from the north at its climatology field. Therefore for anomalies, negative values indicate stronger northerly moisture transport, while positive values represent weaker northerly transport. We calculate the cross-correlation coefficient between the regional mean of precipitation anomalies and regional mean of meridional IVT anomalies in ND, and we find a high negative correlation between them (in Fig. 5), indicating that there is more precipitation in the SESA region when southward water vapor transport is stronger. We select all El Niño years and La Niña years when AAO is at its extreme phases based on Fig. 2. In El Niño (La Niña) years, we calculate the cross-correlation between two climate variability indices (i.e., Niño 3.4 index and SAM index) and meridional IVT anomalies separately. Interestingly, we find that when El Niño occurs, compared to AAO, El Niño plays a more important role in water vapor meridional transport to the SESA region (with higher correlation − 0.57 between Niño 3.4 and IVT, no correlation between AAO and IVT), while during La Niña years, it is the AAO playing a more crucial role in water vapor meridional transport (with correlation coefficient 0.46 between AAO and IVT), while there is no correlation between Niño 3.4 index and IVT anomalies (with a correlation coefficient of − 0.02 between them). This does not mean that during La Niña years, meridional IVT transport is independent of ENSO, but indicates that AAO plays a modulation role among La Niña events, which outperforms the difference among La Niña events.

The composite means of vertical integrated northward water vapor flux anomalies and 850 hPa horizontal wind anomalies within different groups are presented in Fig. 6. From Fig. 6, we see a clear stronger southward moisture flux transport during El Niño years, while this southward moisture flux transport as well as the northerly wind are much weaker in La Niña years, which confirms the previous conclusion that ENSO has linear teleconnection to the precipitation anomalies in SESA. To further explore the impact of AAO, we calculate the difference of composite means in Fig. 6 between different phases of AAO under each ENSO phase. From the results in Fig. 7, we see a pronounced difference between La Niña years combined with different phases of AAO. There is a stronger water vapor flux transported from the north into our study region as well as northerly wind anomalies in La Niña combined with AAO negative phase years (the climatology mean of water vapor flux is

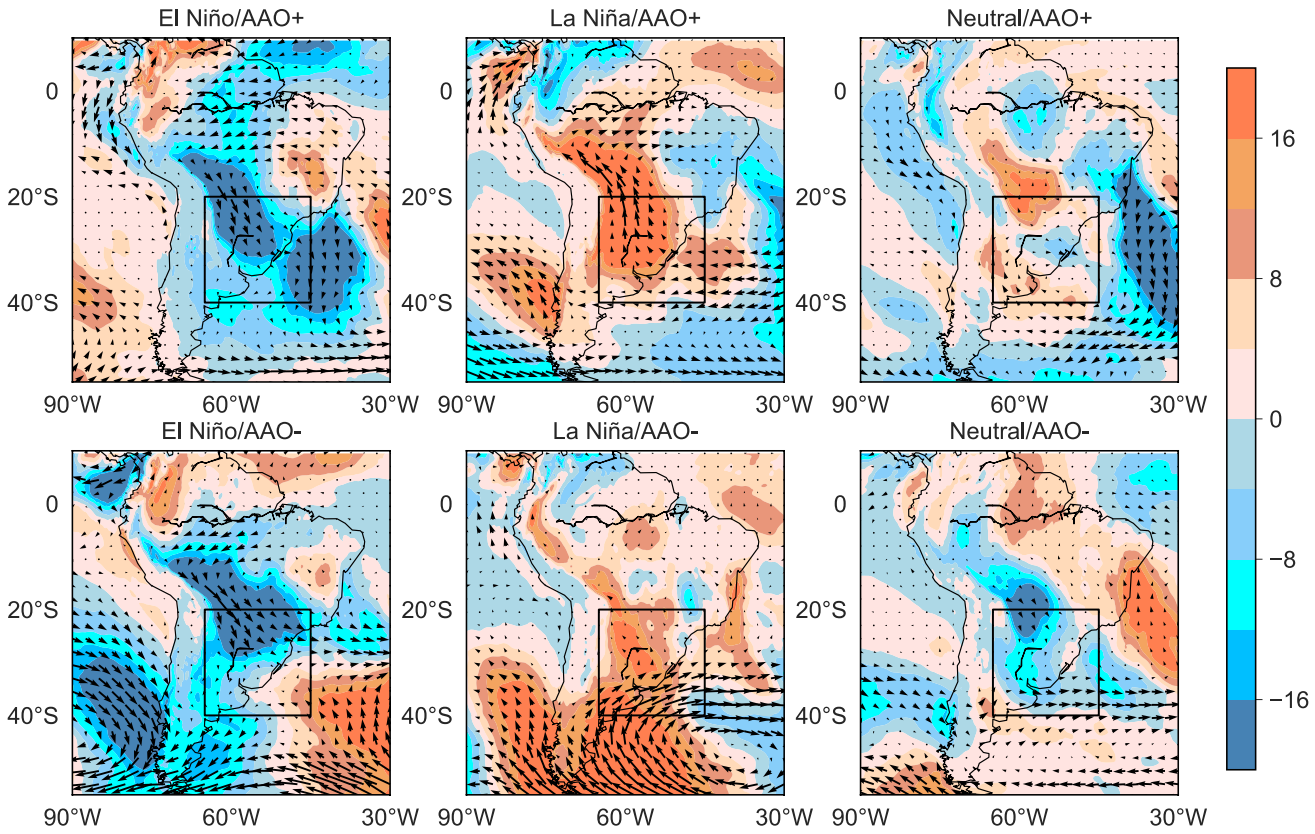

Fig. 6 Composite of vertical integral of northward water vapor flux anomalies (negative values indicate a flux from north to south, unit: kg m^{-1} s^{-1}) and 850 hPa horizontal wind anomalies (vectors, unit: m/s) in different groups

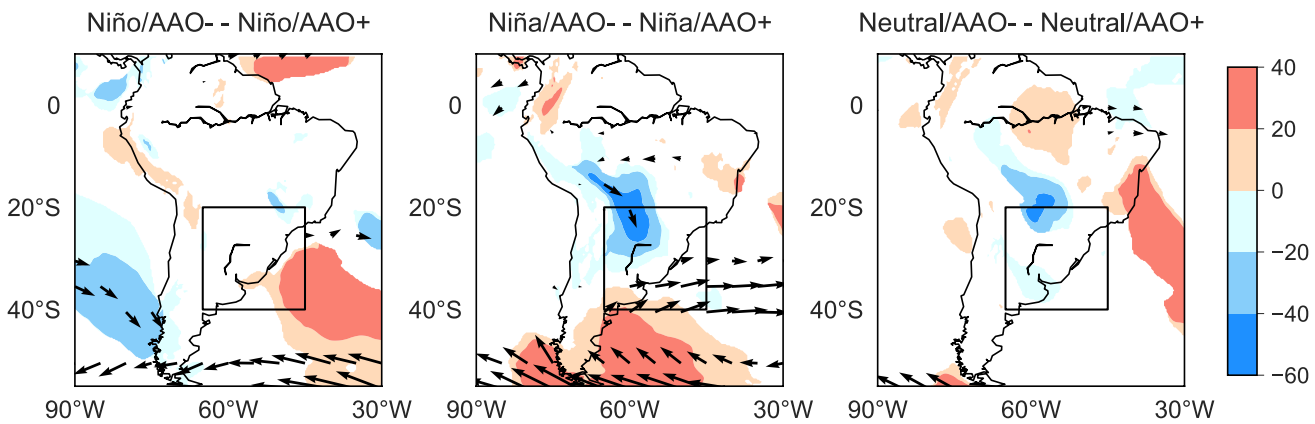

Fig. 7 Difference in composite of northward water vapor flux (negative values indicate a flux from north to south, unit: kg m^{-1} s^{-1}) and 850 hPa horizontal wind (vectors, unit: m/s; only significant results at 90% confidence level according to student's t test are plotted here)

southward, and the low-level wind is northerly wind during La Niña years, in supplementary material, Fig. S1), compared with La Niña combined with AAO positive phase.

3.5 Atmospheric conditions associated with ENSO and AAO

It is known that precipitation anomalies over SESA during ENSO events are associated with atmospheric circulation anomalies (Grimm et al. 2000). According to the results of the previous sections, it is necessary to explore how

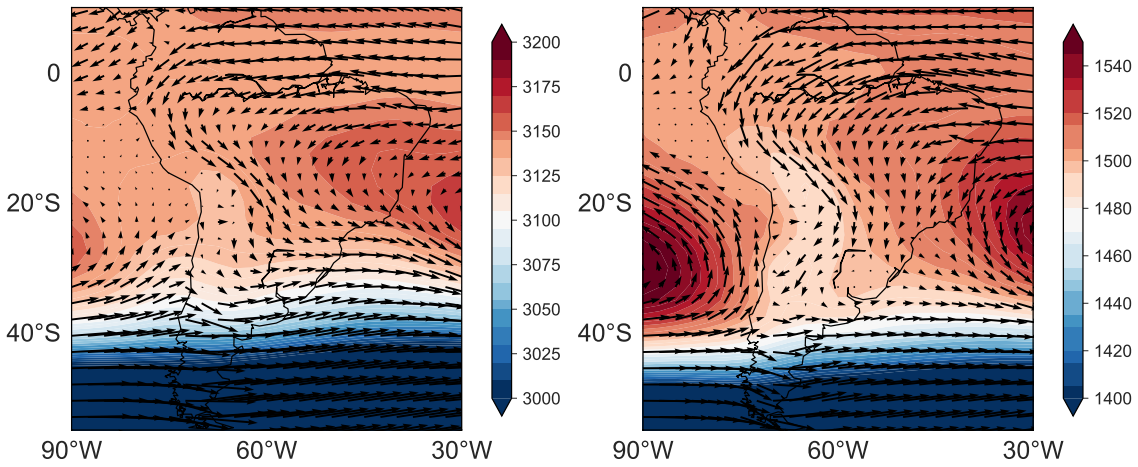

Fig. 8 Climatology of geopotential height (shaded, unit: m) and horizontal wind (unit: m/s) at 700 hPa (left) and 850 hPa (right)

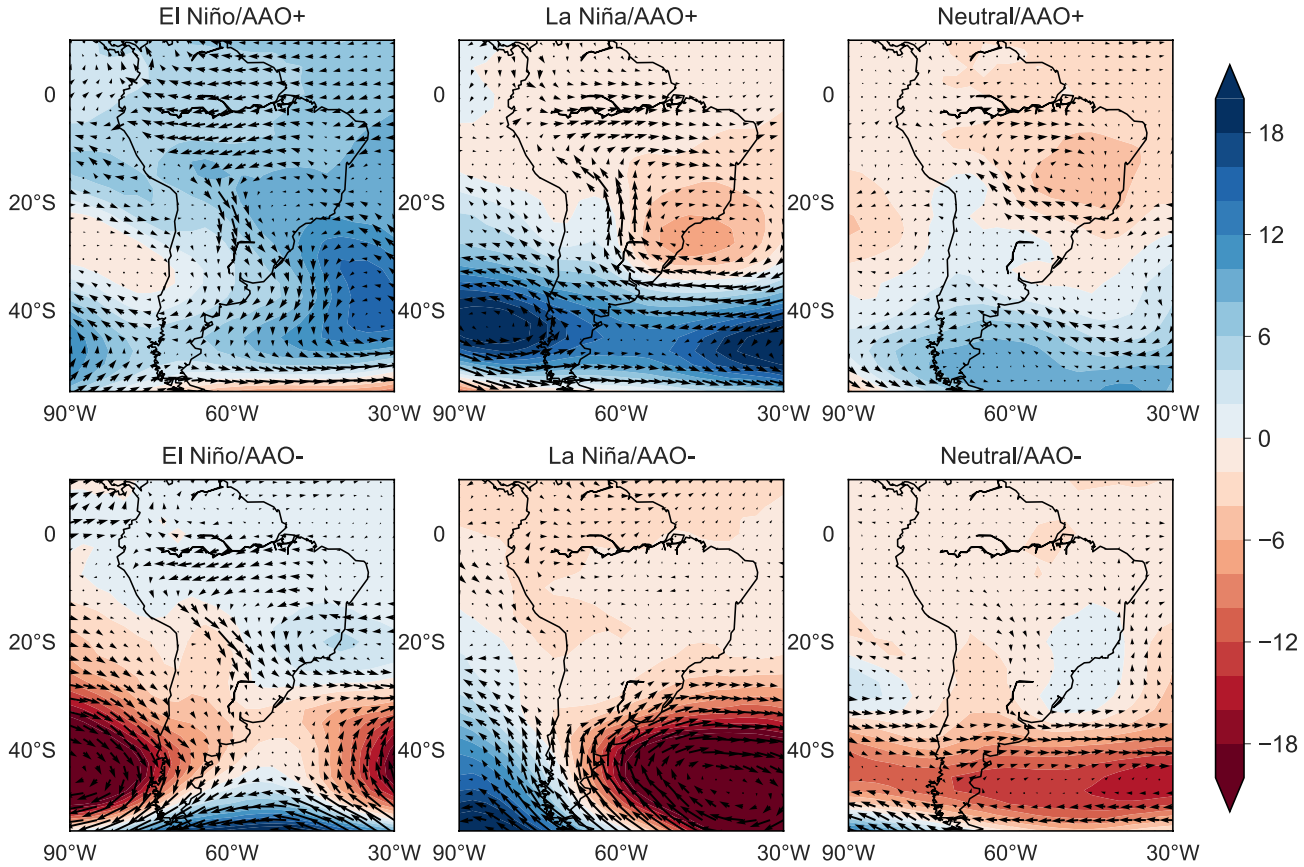

Fig. 9 Composite of geopotential height anomalies (unit: m) and horizontal wind anomalies (unit: m/s) at 700 hPa in different groups

the atmospheric circulation anomalies are associated with ENSO and AAO signals. This section analyzes the atmospheric characteristics related to different phases of ENSO and AAO. From Fig. 8, we can see the Southern Hemisphere subtropical anticyclonic high-pressure systems (also known as Subtropical Anticyclones (SA) or Subtropical highs) in the South Atlantic and South Pacific (refers to the South Atlantic subtropical anticyclone (SASA) and the South Pacific subtropical anticyclone (SPSA) respectively), which connect tropical eateries with midlatitude westerlies (Li

et al. 2013). It is the essential part of the large-scale atmospheric circulation which plays a crucial role in regional precipitation by influencing moisture transport over South America (Doyle and Barros 2002; Fahad et al. 2020). Figure 9 shows that during El Niño years, the SASA strengthens and the northwesterly wind becomes stronger, which is the favoring condition for meridional water vapor transport from northern South America. Previous research concludes that the northeast winds of the South Atlantic subtropical anticyclone (SASA) and the northerly wind of SALLJ provide the convection of moisture from the tropical regions to subtropics and our results are consistent with this conclusion. The Variability of AAO is featured by zonally symmetric patterns of opposite geopotential height anomalies between the pole and the zonal region surrounding latitude 45° S (Gong and Wang 1999). It reflects the intensity variation of the mid-latitude westerly in the Southern Hemisphere (Qin et al. 2005), which causes a permanent influence of extra-tropical disturbances (Quintana and Aceituno 2012). During the positive phase of AAO, the sea level pressure and geopotential height are anomalously high around the mid-latitude, and the migratory low-pressure systems move southward compared to the climatology positions. During the negative phase of the AAO, it favors the lower geopotential height at the mid-latitudes, which is favorable for an intensification of westerlies as well as northward movements of the strongest meridional gradient in sea level pressure and geopotential height. From Fig. 9, AAO's influence on the subtropical region can be seen in each group, especially in La Niña groups, favoring the northerly wind during AAO negative phase. This is consistent with what we mentioned above.

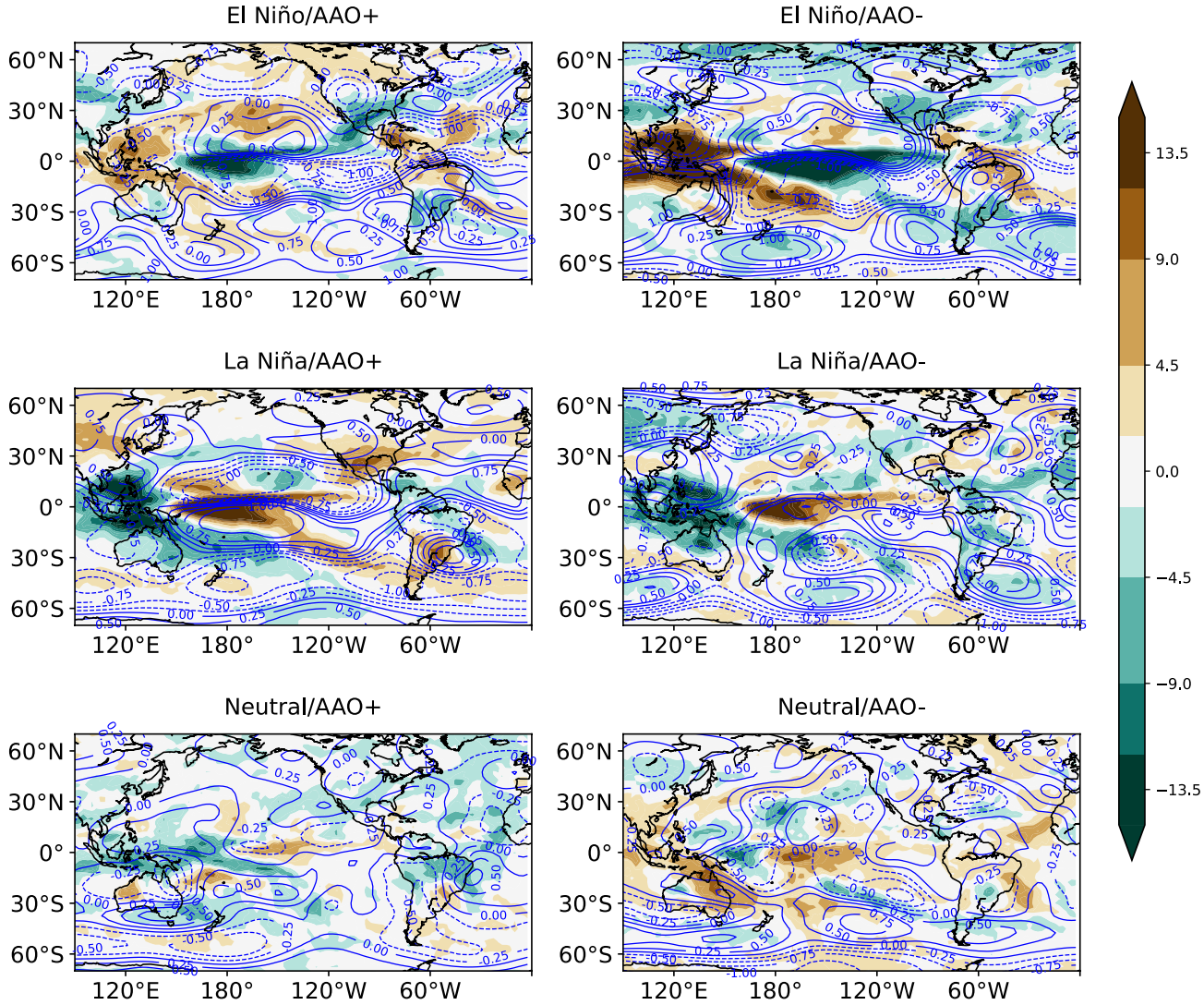

Fig. 10 Composite of stream function at 200 hPa (blue contours, unit: m^2/s) and outgoing longwave radiation (OLR, shading, unit: W/m^2)

Upper-level circulation is also crucial as it provides a dynamic lift for moisture to ascend and generate convection. We look at the upper-level circulation by conducting a composite analysis for 200 hPa streamfunction anomalies. From Fig. 10, we see that during El Niño years, there is an upper-level trough over subtropical South America which indicates the advection of cyclonic vorticity inducing an anomalous increase of precipitation over that region. It is the opposite case during La Niña years, especially for the La Niña/AAO+ case. An upper-level ridge is going against convective development and inducing descent over the SESA region. In Fig. 1, we see that at the low level, the intense trade winds entering northern South America turn southward east of the Andes during all seasons, forming the South America low-level jet (SALLJ) (Zamboni et al. 2010). This meridional flow throughout the year is closely correlated with precipitation east of the Andes at subseasonal and seasonal scales in a way where more (less) rainfall is related to strengthened (weakened) northerly flow (Barros et al. 2002). In other words, the intensity and direction of the SALLJ will decide where and how much it will rain. Precipitation during different seasons is associated with various phenomena, while the SALLJ is a common factor in providing moisture to this region. The SALLJ depends on several phenomena, such as the Amazon convection, the Chaco low, and the regional circulation anomalies induced by ENSO teleconnections. Given that the structure we mentioned in Fig. 10 is barotropic, the anticyclone (cyclone) located to the east of Uruguay helps in strengthening (weakening) the SALLJ during El Niño (La Niña) events. Additionally, in Fig. 10, the OLR anomaly in El Niño groups is negative, illustrating wetter conditions in El Niño groups and vice versa. These patterns are consistent with the results we observe above in terms of precipitation and water vapor flux.

4 Discussion

We also study the impact of eastern pacific (EP) La Niña and central pacific (CP) La Niña events on austral spring precipitation over SESA. We separate different types of La Niña based on the spatial distribution patterns of SST anomalies following the standard raised by Zhang et al. (2015). The EP (CP) La Niña is identified as exhibiting a larger SST anomaly in the east (west) of 150° W during the developing and mature phase of La Niña. The longitude of 150° W is the boundary of Niño 3 (5° S–5° N, 150–90° W) and Niño 4 (5° S–5° N, 160°E–150° W) regions. Compared with the results we obtained above, the difference in impacts of different types of La Niña on precipitation over the SESA region is much weaker compared to the difference in effects of La Niña combined with varying phases of AAO (results are in the supplementary material, Fig. S2). Therefore, AAO can be used as a potential predictor for ENSO's impact on precipitation over this region.

From Section. 3.5, we could conclude that atmospheric patterns associated with different phases of ENSO and AAO can influence the strength of SALLJ, consequently influencing the moisture transported into the SESA region and the precipitation over this area. We also check if AAO and ENSO have an impact on the frequency of SALLJ events. Following the method defined by Montini et al. (2019), we select all the SALLJ days in ND during 1979–2019. Montini et al. conclude that the ERA-Interim 6-hourly dataset outperforms other reanalysis datasets they chose. Therefore we use ERA5 6-hourly zonal and meridional winds at 850 hPa and 700 hPa to detect SALLJ days. SALLJ events are detected based on two locations along the mainstream of the jet, i.e., Santa Cruz de la Sierra, Bolivia (17.8° S, 63.2° W) and Mariscal Estigarribia, Paraguay (22° S, 60.6° W). We follow the criteria defined in that paper: (1) wind speed at 850 hPa exceeding the 75th seasonal percentile, (2) vertical wind shear between 850 hPa and 700 hPa exceeding the 75th seasonal percentile, (3) wind direction is between NW and NE, i.e. meridional component should be larger than the zonal component and meridional wind from the north. We also analyze the influence of ENSO and AAO on SALLJ event frequencies, which is similar to the above settings. We average the SALLJ days each year in every category in Table 1, while we did not see an obvious difference in SALLJ frequencies among different groups. However, the frequency of SALLJ days in El Niño groups and ENSO neutral groups are a bit larger than that in La Niña groups (see in Supplementary material Table I).

5 Conclusion

In this paper, we use composite analysis to explore the combined impact of ENSO and AAO on austral spring precipitation over the SESA region. We conclude that AAO modulates ENSO's teleconnection of austral spring precipitation in this region quite considerably but also nonlinearly: AAO strongly modulates La Niña's impact, with opposite effects on precipitation of AAO negative and positive phases. However, we did not observe this difference for El Niño events indicating that AAO only has a weak impact on SESA during El Niño years. Previous studies indicate that AAO and ENSO have teleconnections to austral spring rainfall over the SESA area, while they only conclude the linear relationship. Our study explores this in a more detailed way to make this topic more complementary.

These observations find their counterparts in our dynamical analysis. For moisture transport, we found that meridional integrated water vapor flux (IVT) contributes most of

the moisture into the SESA region and is highly correlated with the regional precipitation anomalies, confirming that SALLJ plays an essential role in the amount of precipitation in this region. We find that during El Niño years, El Niño plays a vital role in influencing austral spring precipitation over the SESA region, while in La Niña years, AAO outperforms ENSO by its impact on rainfall. For atmospheric circulation, we analyze both low-level and high-level pressure systems, confirming that both, low-level jet transporting moisture and upper-level circulation providing the dynamical lift for moisture, are influenced by ENSO and AAO, leading to different impacts on precipitation over the SESA region. In this paper, we explore the precipitation anomalies within a different combination of AAO and ENSO groups and explain the potential dynamical reason for the precipitation patterns we observe. The mechanisms of how AAO leads to the difference in circulation systems are beyond this paper's scope and need further work in the future.

Supplementary Information The online version contains supplementary material available at https://doi.org/10.1007/s00382-022-06592-8.

Acknowledgements This work is part of the Climate Advanced Forecasting of sub-seasonal Extremes (CAFE) which has received funding from the European Union's Horizon 2020 research and innovation programme under the Marie Skłodowska-Curie grant agreement No. 813844.

Author contributions All authors contributed to the conception and design of this research. Data analysis programming and figure plotting were performed by Xinjia Hu. Suggestions for the statistical analysis were provided by Jan Eichner. Suggestions for the structure of the manuscript and AAO-related dynamical analysis were provided by Daoyi Gong. The dynamical analysis for the SESA region was provided by Marcelo Barreiro. The manuscript was written by Xinjia Hu and Holger Kantz. The project was led by Holger Kantz and the manuscript was revised by Holger Kantz.

Funding Open Access funding enabled and organized by Projekt DEAL. This project has received funding from the European Union's Horizon 2020 research and innovation programme under the Marie Skłodowska-Curie grant agreement No. 813844.

Data availability The data used in this study are publicly available online.

Code availability Not applicable.

Declarations

Conflict of interest The authors declare that they have no conflict of interest.

Open Access This article is licensed under a Creative Commons Attribution 4.0 International License, which permits use, sharing, adaptation, distribution and reproduction in any medium or format, as long as you give appropriate credit to the original author(s) and the source, provide a link to the Creative Commons licence, and indicate if changes were made. The images or other third party material in this article are included in the article's Creative Commons licence, unless indicated otherwise in a credit line to the material. If material is not included in the article's Creative Commons licence and your intended use is not permitted by statutory regulation or exceeds the permitted use, you will need to obtain permission directly from the copyright holder. To view a copy of this licence, visit http://creativecommons.org/licenses/by/4.0/.

References

Adler RF, Sapiano MR, Huffman GJ, Wang JJ, Gu G, Bolvin D, Chiu L, Schneider U, Becker A, Nelkin E et al (2018) The global precipitation climatology project (GPCP) monthly analysis (new version 2.3) and a review of 2017 global precipitation climatology project (GPCP) monthly analysis (new version 2.3) and a review of 2017 global precipitation. Atmosphere 9(4):138. https://doi.org/10.3390/atmos9040138

Alexander LV, Bador M, Roca R, Contractor S, Donat MG, Nguyen PL (2020) Intercomparison of annual precipitation indices and extremes over global land areas from in situ, space-based and reanalysis products. Environ Res Lett 15(5):055002. https://doi.org/10.1002/joc.6643

Barreiro M (2010) Influence of ENSO and the south Atlantic ocean on climate predictability over southeastern South America. Clim Dyn 35(7):1493–1508. https://doi.org/10.1007/s00382-009-0666-9

Barros VR, Silvestri GE (2002) The relation between sea surface temperature at the subtropical south-central Pacific and precipitation in southeastern South America. J Clim 15(3):251–267. https://doi.org/10.1175/1520-0442(2002)015<0251:TRBSST>2.0.CO;2

Barros VR, Grimm AM, Doyle ME (2002) Relationship between temperature and circulation in southeastern South America and its influence from El Ninño and La Ninña events. J Meteorol Soc Jpn Ser II 80(1):21–32. https://doi.org/10.2151/jmsj.80.21

Clem KR, Fogt RL (2013) Varying roles of ENSO and SAM on the Antarctic peninsula climate in austral spring. J Geophys Res Atmos 118(20):11–481. https://doi.org/10.1002/jgrd.50860

de Souza IP, Andreoli RV, Kayano MT, Vargas FF, Cerón WL, Martins JA, Freitas E, de Souza RAF (2021) Seasonal precipitation variability modes over South America associated to El Niño-southern oscillation (ENSO) and non-ENSO components during the 1951–2016 period. Int J Climatol 41(8):4321–4338. https://doi.org/10.1002/joc.7075

Díaz LB, Saurral RI, Vera CS (2021) Assessment of South America summer rainfall climatology and trends in a set of global climate models large ensembles. Int J Climatol 41:E59–E77. https://doi.org/10.1002/joc.6643

Doyle ME, Barros VR (2002) Midsummer low-level circulation and precipitation in subtropical South America and related sea surface temperature anomalies in the South Atlantic. J Clim 15(23):3394–3410. https://doi.org/10.1175/1520-0442(2002)015<3394:MLLCAP>2.0.CO;2

Fahad AA, Burls NJ, Strasberg Z (2020) How will southern hemisphere subtropical anticyclones respond to global warming? Mechanisms and seasonality in CMIP5 and CMIP6 model projections. Clim Dyn 55(3):703–718. https://doi.org/10.1007/s00382-020-05290-7

Fogt RL, Bromwich DH (2006) Decadal variability of the ENSO teleconnection to the high-latitude South Pacific governed by coupling with the southern annular mode. J Clim 19(6):979–997. https://doi.org/10.1175/JCLI3671.1

Fogt RL, Bromwich DH, Hines KM (2011) Understanding the SAM influence on the South Pacific ENSO teleconnection. Clim Dyn 36(7):1555–1576. https://doi.org/10.1007/s00382-010-0905-0

Gong D, Wang S (1999) Definition of Antarctic oscillation index. Geophys Res Lett 26(4):459–462. https://doi.org/10.1029/1999GL900003

Gong T, Feldstein SB, Luo D (2010) The impact of ENSO on wave breaking and southern annular mode events. J Atmos Sci 67(9):2854–2870. https://doi.org/10.1175/2010JAS3311.1

Gonzalez PL, Polvani LM, Seager R, Correa GJ (2014) Stratospheric ozone depletion: a key driver of recent precipitation trends in south eastern South America. Clim Dyn 42(7):1775–1792. https://doi.org/10.1007/s00382-013-1777-x

Grimm AM, Ferraz SE, Gomes J (1998) Precipitation anomalies in Southern Brazil associated with El Niño and La Niña events. J Clim 11(11):2863–2880. https://doi.org/10.1175/1520-0442(1998)011<2863:PAISBA>2.0.CO;2

Grimm AM, Barros VR, Doyle ME (2000) Climate variability in southern South America associated with El Niño and La Niña events. J Clim 13(1):35–58. https://doi.org/10.1175/1520-0442(2002)015<3394:MLLCAP>2.0.CO;2

Han T, Wang H, Sun J (2017) Strengthened relationship between the Antarctic oscillation and ENSO after the mid-1990s during austral spring. Adv Atmos Sci 34(1):54–65. https://doi.org/10.1007/s00376-016-6143-6

Harris I, Osborn TJ, Jones P, Lister D (2020) Version 4 of the CRU TS monthly high-resolution gridded multivariate climate dataset. Sci Data 7(1):1–18. https://doi.org/10.1038/s41597-020-0453-3

Hersbach H, Bell B, Berrisford P, Biavati G, Horányi A, Muñoz Sabater J, Nicolas J, Peubey C, Radu R, Rozum I et al (2019) Era5 monthly averaged data on single levels from 1979 to present. Copernicus Climate Change Service (C3S) Climate Data Store (CDS) 10:252–266

Hersbach H, Bell B, Berrisford P, Hirahara S, Horányi A, Muñoz-Sabater J, Nicolas J, Peubey C, Radu R, Schepers D et al (2020) The ERA5 global reanalysis. Q J R Meteorol Soc 146(730):1999–2049. https://doi.org/10.1002/qj.3803

Kalnay E, Kanamitsu M, Kistler R, Collins W, Deaven D, Gandin L, Iredell M, Saha S, White G, Woollen J et al (1996) The NCEP/NCAR 40-year reanalysis project. Bull Am Meteorol Soc 77(3):437–472. https://doi.org/10.1175/1520-0477(1996)077<0437:TNYRP>2.0.CO;2

L'Heureux ML, Thompson DW (2006) Observed relationships between the El Niño-southern oscillation and the extratropical zonal-mean circulation. J Clim 19(2):276–287. https://doi.org/10.1175/JCLI3617.1

Li W, Li L, Ting M, Deng Y, Kushnir Y, Liu Y, Lu Y, Wang C, Zhang P (2013) Intensification of the southern hemisphere summertime subtropical anticyclones in a warming climate. Geophys Res Lett 40(22):5959–5964. https://doi.org/10.1002/2013GL058124

Liebmann B, Smith CA (1996) Description of a complete (interpolated) outgoing longwave radiation dataset. Bull Am Meteorol Soc 77(6):1275–1277. https://www.jstor.org/stable/26233278?seq=1

Marshall GJ (2003) Trends in the southern annular mode from observations and reanalyses. J Clim 16(24):4134–4143. https://doi.org/10.1175/1520-0442(2003)016<4134:TITSAM>2.0.CO;2

Martín-Gómez V, Barreiro M (2016) Analysis of oceans' influence on spring time rainfall variability over southeastern South America during the 20th century. Int J Climatol 36(3):1344–1358. https://doi.org/10.1002/joc.4428

Mo KC, Paegle JN (2001) The Pacific-South American modes and their downstream effects. Int J Climatol 21(10):1211–1229. https://doi.org/10.1002/joc.685

Montecinos A, Díaz A, Aceituno P (2000) Seasonal diagnostic and predictability of rainfall in subtropical South America based on tropical Pacific SST. J Clim 13(4):746–758. https://doi.org/10.1175/1520-0442(2000)013<0746:SDAPOR>2.0.CO;2

Montini TL, Jones C, Carvalho LM (2019) The South American low-level jet: a new climatology, variability, and changes. J Geophys Res Atmos 124(3):1200–1218. https://doi.org/10.1029/2018JD029634

Nuñez MN, Blázquez J (2014) Climate change in La Plata basin as seen by a high-resolution global model. Atmos Clim Sci 4:272–289. https://doi.org/10.4236/acs.2014.42029

Olmo ME, Bettolli ML (2022) Statistical downscaling of daily precipitation over southeastern South America: assessing the performance in extreme events. Int J Climatol 42(2):1283–1302. https://doi.org/10.1002/joc.7303

Olmo M, Bettolli ML, Rusticucci M (2020) Atmospheric circulation influence on temperature and precipitation individual and compound daily extreme events: spatial variability and trends over southern South America. Weather Clim Extremes 29:100267. https://doi.org/10.1016/j.wace.2020.100267

Qin J, Px Wang, Gong Y (2005) Impacts of Antarctic oscillation on summer moisture transport and precipitation in eastern china. Chin Geogr Sci 15(1):22–28. https://doi.org/10.1007/s11769-003-0064-x

Quintana J, Aceituno P (2012) Changes in the rainfall regime along the extratropical west coast of South America (Chile): 30–43S. Atmósfera 25(1):1–22

Rao V, Hada K (1990) Characteristics of rainfall over Brazil: annual variations and connections with the southern oscillation. Theor Appl Climatol 42(2):81–91. https://doi.org/10.1007/BF00868215

Ropelewski CF, Halpert MS (1987) Global and regional scale precipitation patterns associated with the El Niño/southern oscillation. Mon Weather Rev 115(8):1606–1626. https://doi.org/10.1175/1520-0493(1987)115<1606:GARSPP>2.0.CO;2

Salio P, Nicolini M, Saulo AC (2002) Chaco low-level jet events characterization during the austral summer season. J Geophys Res Atmos 107(D24):ACL 32-1-ACL 32-17. https://doi.org/10.1029/2001JD001315

Satyamurty P, da Costa CPW, Manzi AO (2013) Moisture source for the amazon basin: a study of contrasting years. Theor Appl Climatol 111(1):195–209. https://doi.org/10.1007/s00704-012-0637-7

Schneider U, Fuchs T, Meyer-Christoffer A, Rudolf B (2008) Global precipitation analysis products of the GPCC. Global Precipitation Climatology Centre (GPCC), DWD, Internet Publikation 112

Schneider U, Finger P, Meyer-Christoffer A, Rustemeier E, Ziese M, Becker A (2017) Evaluating the hydrological cycle over land using the newly-corrected precipitation climatology from the global precipitation climatology centre (gpcc). Atmosphere 8(3):52. https://doi.org/10.3390/atmos8030052

Schneider U, Becker A, Finger P, Rustemeier E, Ziese M (2020) GPCC full data monthly product version 2020 at 0.25°: monthly land-surface precipitation from rain-gauges built on GTS-based and historical data. https://doi.org/10.5676/DWD_GPCC/FD_M_V2020_025

Silvestri GE (2005) Comparison between winter precipitation in southeastern South America during each ENSO phase. Geophys Res Lett 32(5). https://doi.org/10.1029/2004GL021749

Silvestri GE, Vera CS (2003) Antarctic oscillation signal on precipitation anomalies over southeastern South America. Geophys Res Lett 30(21). https://doi.org/10.1029/2003GL018277

Stammerjohn SE, Martinson D, Smith R, Yuan X, Rind D (2008) Trends in Antarctic annual sea ice retreat and advance and their relation to El Niño–southern oscillation and southern annular mode variability. J Geophys Res Oceans 113(C3). https://doi.org/10.1029/2007JC004269

Thompson DW, Wallace JM (2000) Annular modes in the extratropical circulation. Part I: month-to-month variability. J Clim 13(5):1000–1016. https://doi.org/10.1175/1520-0442(2000)013<1000:AMITEC>2.0.CO;2

Vasconcellos FC, Cavalcanti IF (2010) Extreme precipitation over southeastern brazil in the austral summer and relations with the southern hemisphere annular mode. Atmos Sci Lett 11(1):21–26. https://doi.org/10.1002/asl.247

Vera CS, Osman M (2018) Activity of the southern annular mode during 2015–2016 El Niño event and its impact on southern hemisphere climate anomalies. Int J Climatol 38:e1288–e1295. https://doi.org/10.1002/joc.5419

Vera CS, Alvarez MS, Gonzalez PL, Liebmann B, Kiladis GN (2018) Seasonal cycle of precipitation variability in South America on intraseasonal timescales. Clim Dyn 51(5):1991–2001. https://doi.org/10.1007/s00382-017-3994-1

Virji H (1981) A preliminary study of summertime tropospheric circulation patterns over South America estimated from cloud winds. Mon Weather Rev 109(3):599–610. https://doi.org/10.1175/1520-0493(1981)109<0599:APSOST>2.0.CO;2

Xie P, Arkin PA (1997) Global precipitation: a 17-year monthly analysis based on gauge observations, satellite estimates, and numerical model outputs. Bull Am Meteorol Soc 78(11):2539–2558. https://doi.org/10.1175/1520-0477(1997)078<2539:GPAYMA>2.0.CO;2

Zamboni L, Mechoso CR, Kucharski F (2010) Relationships between upper-level circulation over South America and rainfall over southeastern South America: a physical base for seasonal predictions. J Clim 23(12):3300–3315. https://doi.org/10.1175/2009JCLI3129.1

Zhang W, Wang L, Xiang B, Qi L, He J (2015) Impacts of two types of La Niña on the Nao during boreal winter. Clim Dyn 44(5):1351–1366. https://doi.org/10.1007/s00382-014-2155-z

Publisher's Note Springer Nature remains neutral with regard to jurisdictional claims in published maps and institutional affiliations.